Four Decades of Research on Massive Stars
ASP Conference Series, Vol. 465
Laurent Drissen, Carmelle Robert, Nicole St-Louis, and Anthony F. J. Moffat, eds.

Hyperspectral Imagers for the Study of Massive Star Nebulae

Laurent Drissen, Alexandre Alarie, Thomas Martin, and the SpIOMM/SITELLE Team

Département de physique, de génie physique et d'optique, Université Laval 1045 avenue de la médecine, Québec, QC, Canada

Abstract. We present two wide-field imaging Fourier transform spectrometers built by our team to study the interstellar medium around massive stars in the Milky Way and nearby galaxies. SpIOMM, attached to the Mont Mégantic 1.6-m telescope, is capable of obtaining the visible spectrum of every source of light in a 12 arcminute field of view, with a spectral resolution ranging from R = 1 (wide-band image) to R = 25 000, resulting in about a million spectra with a spatial resolution of one arcsecond. SITELLE will be a similar instrument attached to the Canada-France-Hawaii telescope, and will be in operation in early 2013. We illustrate SpIOMM's capabilities to study the interactions between massive stars and their environment.

1. Lessons Learned

Those of us who were fortunate enough to work under Tony's supervision during their graduate years learned a lot from him. We learned, of course, to love massive stars and to appreciate their immense efforts to light up and enrich the Universe. We also learned that astronomy is fun and that we would never be bored by our job. But one thing I will always remember from spending so many observing nights with Tony is that light coming from those nearby stars and distant galaxies is an invaluable source of information that must be exploited as much as possible. We learned the mysteries of photometry, polarimetry, photographic plates and the first generations of CCDs; spectroscopy of course, sometimes observing at airmasses approaching 3.3 just above the three tops; and spectropolarimetry. All that from the X-rays to the radio! It is with these lessons in mind that I have spent the past decade developing, with my students and colleagues, hyperspectral imagers allowing us to obtain a spectrum of every single source of light in wide fields of view.

2. Imaging Fourier Transform Spectrometers

While Fourier Transform Spectrometers (FTS) are widely used in remote sensing, atmospheric analysis and chemical applications, as well as planetary exploration (on board the Mariner, Voyager and more recently Cassini spacecrafts - see for instance Flasar et al. (2004)), the use of FTS is not widespread in astronomy, mostly because of the technical difficulties in building such instruments, especially in the visible range. We must however mention the BEAR imaging FTS (Chaufray et al. 2011), which provided a 24″ field of view in the near infrared at the CFHT in the 1990's, and the more

recent imaging FTS mode of the SPIRE instrument onboard the Herschel space telescope (Rangwala et al. 2011).

With an imaging FTS, spectral information is obtained by acquiring multiple panchromatic images of the selected scene that are modulated in intensity in a precisely controlled fashion. The core of the instrument is a Michelson interferometer inserted in series within the camera optical design, which modulates the image intensity from total dark to total brightness depending on the optical path difference (OPD) between the two interferometer arms. This OPD being a function of wavelength, the resulting image intensity is the sum of all individual wavelength contributions. A recording of these panchromatic images generated at equally spaced OPD positions creates the raw data cube, thus producing a discrete interferogram for each pixel of the image from which spectral information can then be extracted. The spectrum of the source, at each pixel, is obtained from the Fourier transform of these individual interferograms. The net results are thus a deep panchromatic image of the target and a complete set of spectra, one for every pixel.

From our point of view, the niche of an astronomical IFTS clearly sits in the wide field coverage, moderate spectral resolution (R $\sim$ 2000 – 10000) and the large waveband coverage, although it is interesting to note that the FTS was classically known for its ability to obtain very high spectral resolution of the targets. Two important advantages of an imaging FTS are its intrinsically high throughput (only mirrors and lenses are used, like in imagers; no gratings nor optical fibers like in dispersive Integral Field Spectrometers) and the fact that, contrary to conventional IFUs, no image reconstruction is necessary. The enormous advantages of a wide-field imaging FTS over traditional, dispersive spectrometers, especially for the study of emission-line objects and for cosmological studies, have been described by Bennett (2000) in the context of the then-called Next Generation Space Telescope (now the James Webb Space Telescope).

3. SpIOMM and SITELLE

SpIOMM, an imaging FTS with a $12' \times 12'$ field of view, was designed, built and improved over the years by a very talented group of students at Université Laval (Grandmont et al. 2003; Drissen et al. 2008; Bernier et al. 2008) in collaboration with a Québec-based company, ABB-Bomem. SpIOMM, which is attached to the 1.6-m telescope of the Observatoire du mont Mégantic, is capable of obtaining hyperspectral data cubes in selected wavebands of the visible (350 - 850 nm), with a spectral resolution ranging from R = 1 (wide-band image) to R = 25 000, resulting in about a million spectra with a spatial resolution limited by the seeing. We have mostly used SpIOMM with R 2000 in a blue (450 - 520 nm) and a red (650 - 680 nm) wavebands, encompassing the following emission lines: Hβ, Hα, [OIII] $\lambda\lambda$4959, 5007, [NII] $\lambda\lambda$6548, 6584, [SII]$\lambda\lambda$6717, 6731 and He I λ6678. Until recently, SpIOMM used only one of its two output ports, equipped with a 1300×1300 pixel Princeton Scientific CCD camera; but we have recently installed a second camera (2048×2048 Apogee) on the second output port; this not only doubles the flux but also allows us to easily correct the interferograms for any transparency variations during the exposure.

Apart from its image quality and overall transmission efficiency, which are common to all astronomical instruments, the performance of an FTS is characterized by its modulation efficiency (ME), which is the capability of the interferometer to modulate the incident light. This parameter, which can be viewed as an analog to the

grating efficiency in dispersive spectrographs, depends on a multitude of factors but most specifically on the surface quality and the alignment of the optical components. The main technical challenge of such instruments is therefore to be able to maintain the desired distance and alignment between the two mirrors of the interferometer in a very hostile environment (changing wind, temperature, gravity vector, vibrations from the telescope, ...). The smallest angle deviation from a perfect alignment between the two mirrors reduces the spatial coherence (interference) of the two beams as they recombine. This effect is more obvious at short wavelengths. A deviation of only 1.5 microradian from perfect alignment can decrease the ME by up to 25% at 350 nm. Stability of the optical path difference between the two arms of the interferometer during an exposure is also essential. An OPD jitter with a standard deviation of 10 nm typically reduces ME by about 2%. SpIOMM's ME reaches $\sim$ 85% at 650 nm, but only $\sim$ 20% at 350 nm.

SpIOMM is a prototype installed on a relatively small aperture telescope, but our team is currently working on SITELLE, a similar instrument to be installed at the Canada-France-Hawaii telescope in 2013 (Drissen et al. 2010). SITELLE will be much more robust and efficient than SpIOMM, in particular in the near UV (350 nm) where ME is expected to reach 70%.

4. Science Cases

While the number of scientific applications of wide-field hyperspectral imagers is potentially very large, our group has focused on the interstellar medium of the Milky way and nearby spiral galaxies. A meaningful link between local heavy element enrichment and the global chemical evolution of galaxies can only be established by detailed studies of individual wind-blown bubbles in our own galaxy. Winds of evolved massive stars and their surrounding bubbles (LBVs and Wolf-Rayet ejecta, supernova remnants) are known to be globally enriched with products of nucleosynthesis. A complete survey of abundance, density, temperature and kinematic measurements with full spatial coverage of nebulae surrounding individual massive stars, ionizing clusters up to the diffuse ISM of galaxies, looking for inhomogeneities in the distribution of processed material will provide firm grounds for the interpretation of global galactic abundance studies.

We have therefore obtained data cubes of O-star and Wolf-Rayet nebulae (such as NGC 7635 and NGC 6888), Galactic supernova remnants (the Cygnus Loop, the Crab and Cas A), as well as ionized regions of nearby galaxies (such as M31 and NGC 1569). We briefly describe below some preliminary results on the supernova remnants.

4.1. The Cygnus Loop

We have begun a complete mapping of the Cygnus Loop, a 15 000 year-old supernova remnant spanning many degrees in the sky, in order to characterize this important object in its entirety. Although the Cygnus Loop has been observed at many wavelengths, a complete spectroscopic coverage in the visible range is still missing. Fig. 1 depicts some characteristics of a single red data cube, showing the unusually strong [SII] lines. This cube illustrates that SpIOMM can be used at the same time as an imager with a set of perfect narrow-band filters as well as a medium-resolution, wide field spectrograph. Although the observed Doppler shifts are not as extreme as those of younger SNRs (see below), they are sufficient in most regions of the Cygnus Loop to allow us to disentangle

filaments which spatially overlap in the line of sight. A detailed analysis of these data is underway (A. Alarie's Ph. D. thesis).

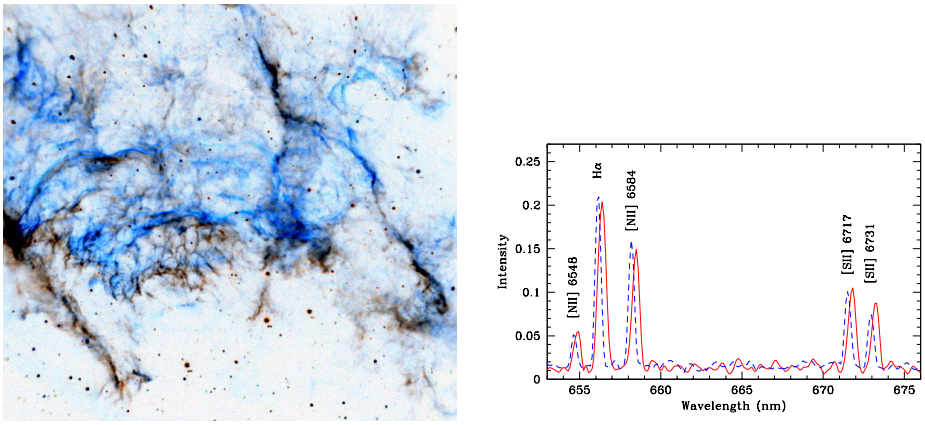

Figure 1. Composite image of a 12′ × 12′ section of NGC 6992, from Hα and [NII] images extracted from a red (650 - 680 nm) SpIOMM data cube. On the right, example of spectrograms from two filaments with different velocities; each is an average of five pixels (out of the 500 000 from the cube).

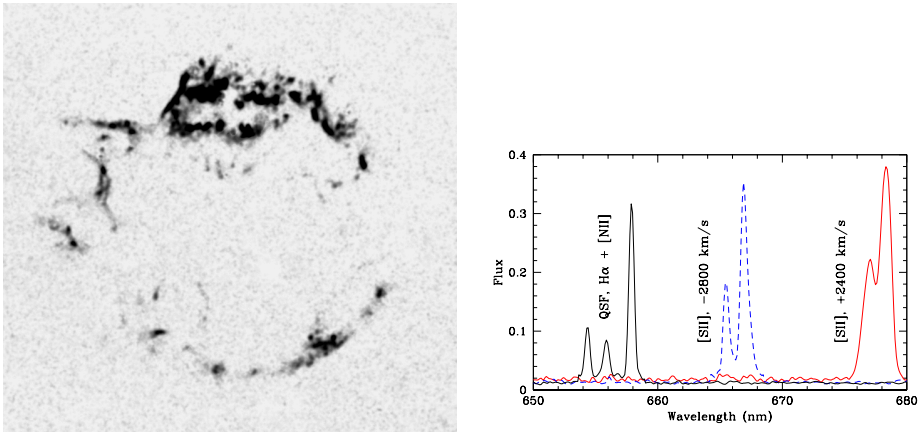

Figure 2. Composite image of Cas A from [SII] and [OIII] images extracted from SpIOMM data cubes. On the right, we have superimposed spectra of three knots: a nitrogen-rich *Quasi-Stationary Floculus* (QSF), resulting from the interaction between the pre-supernova wind and the SN shock wave; and two sections of rapidly expanding filaments with very high electron density (as can be seen by the "inverted" ratio of the [SII] doublet lines; compare with Fig. 1).

4.2. The Crab and Cas A

The case of two much younger supernova remnant, M1 (the Crab nebula), and Cas A are particularly interesting as they illustrate the full power of SpIOMM. A few cen-

turies after the explosions, the gas is still globally expanding today at velocities of up to 1500 km/s in the case of M1 and more than 3000 km/s for Cas A, causing very strong Doppler shifts. Moreover, because of the presence of shocks, the forbidden lines of [NII] $\lambda\lambda$6548, 6584 and [SII] $\lambda\lambda$6717, 6731 are almost as strong as the (usually strongest) Hα. Therefore, up to ten strong emission lines can be seen in spectra of regions where two approaching and receding filaments are superimposed on the line of sight.

Charlebois et al. (2010) presented a detailed analysis of the M1 data cubes. The truly novel aspect of these data is that they allowed us to derive a reliable tridimensional photoionization and electronic density maps of this supernova remnant which imply strong constraints for any model that aims at a deeper understanding of the emission processes at play in the Crab. In particular, the ionization process and the density structure distribution have been deduced and both show a clear strong NW-SE asymmetry, and reveal that the skin-less NW lobe appears to have evolved faster than the SE part. These characteristics are possibly related to a fundamental asymmetry in the explosion mechanism itself.

Cas A, the result of a type IIb SN explosion (Krause et al. 2008), is even younger than M1 and therefore displays even larger expansion velocities (see Fig. 2). It has been known for a long time that structures with radically different spectroscopic and kinematical properties cohabit in this object (Chevalier & Kirshner 1978), revealing the complex interaction between the supernova and its progenitor's wind. Two data cubes of Cas A with SpIOMM (Fig. 2), combined with multi-epoch archival images obtained with the *Hubble Space Telescope* allowed us to determine the three dimensional structure of this object. Details of this analysis will be published elsewhere.

Acknowledgments. We thank NSERC and FQRNT for funding. SpIOMM and SITELLE, funded by the Canadian Foundation for Innovation, are collaborations between Université Laval and ABB-Bomem.

References

Bennett, C. L. 2000, in Next Generation Space Telescope Science and Technology, edited by E. Smith & K. Long, vol. 207 of ASP Conf. Series, 344

Bernier, A.-P., Charlebois, M., Drissen, L., & Grandmont, F. 2008, in Ground-based and Airborne Instrumentation for Astronomy II, vol. 7014 of SPIE Conf. Series, 70147J

Charlebois, M., Drissen, L., Bernier, A.-P., Grandmont, F., & Binette, L. 2010, AJ, 139, 2083

Chaufray, J.-Y., Greathouse, T. K., Gladstone, G. R., et al. 2011, Icarus, 211, 1233

Chevalier, R. A., & Kirshner, R. P. 1978, ApJ, 219, 931

Drissen, L., Bernier, A.-P., Charlebois, M., et al. 2008, in Ground-based and Airborne Instrumentation for Astronomy II, vol. 7014 of SPIE Conf. Series, 70147K

Drissen, L., Bernier, A.-P., Rousseau-Nepton, L., et al. 2010, in Ground-based and Airborne Instrumentation for Astronomy III, vol. 7735 of SPIE Conf. Series, 77350B

Flasar, F. M., Kunde, V. G., Abbas, M. M., et al. 2004, Space Sci.Rev., 115, 169

Grandmont, F., Drissen, L., & Joncas, G. 2003, in Specialized Optical Developments in Astronomy, edited by E. Atad-Ettedgui & S. D'Odorico, vol. 4842 of SPIE Conf. Series, 392

Krause, O., Birkmann, S. M., Usuda, T., et al. 2008, Science, 320, 1195

Rangwala, N., Maloney, P. R., Glenn, J., et al. 2011, ApJ, 743, 94

Discussion

Bomans: I remember that there used to be a problem with the signal-to-noise ratio with FTS in the past. How did you solve this?

Drissen: Actually, the peculiarity you mention, inherent to all FTS, comes from the fact that at each step in the data cube, the entire waveband is acquired (you do not "scan" the line as in a Fabry-Perot, for example) and therefore the photon noise at each wavelength comes from the entire bandpass. This can become a problem for continuum sources with absorption lines, where most of the flux (and therefore the noise) comes from (the continuum) outside the wavelength of interest - the lines themselves. This is why a dispersive spectrograph will always be more efficient than an FTS to get spectra of faint individual (or small number of) stars. On the other hand, an imaging FTS becomes competitive with dispersive spectrographs for extended objects with continuum and absorption lines and is unbeatable in the case of extended emission-line objects such as nebulae and late-type galaxies.

Sana: I want to do 30 Dor with that instrument! Is it possible to move it to the southern hemisphere?

Drissen: SpIOMM can be attached to any f/8 telescope with a Cassegrain bonnette.

Eversberg: In order to get your 3D view of Cas A, you must have assumed a model for the expansion of the nebula.

Drissen: Indeed, the third dimension displayed in the animation was the line-of-sight velocity, not the real distance from us.

Jean-Michel Mugnès, Laurent Drissen, Carmelle Robert, André-Nicolas Chené and Christopher Russell geting ready for the rabaska excursion